

Droplet Microarray Based Screening Identifies Proteins for Maintaining Pluripotency of hiPSCs

Yanxi Liu, Sarah Bertels, Markus Reischl, Ravindra Peravali, Martin Bastmeyer, Anna A. Popova, and Pavel A. Levkin*


Human induced pluripotent stem cells (hiPSCs) are crucial for disease modeling, drug discovery, and personalized medicine. Animal-derived materials hinder applications of hiPSCs in medical fields. Thus, novel and well-defined substrate coatings capable of maintaining hiPSC pluripotency are important for advancing biomedical applications of hiPSCs. Here a miniaturized droplet microarray (DMA) platform to investigate 11 well-defined proteins, their 55 binary and 165 ternary combinations for their ability to maintain pluripotency of hiPSCs when applied as a surface coating, is used. Using this screening approach, ten protein group coatings are identified, which promote significantly higher *NANOG* expression of hiPSCs in comparison with Matrigel coating. With two of the identified coatings, long-term pluripotency maintenance of hiPSCs and subsequent differentiation into three germ layers are achieved. Compared with conventional high-throughput screening (HTS) in 96-well plates, the DMA platform uses only 83 μL of protein solution (0.83 μg total protein) and only $\approx 2.8 \times 10^5$ cells, decreasing the amount of proteins and cells ≈ 860 and 25-fold, respectively. The identified proteins will be essential for research and applications using hiPSCs, while the DMA platform demonstrates great potential for miniaturized HTS of scarce cells or expensive materials such as recombinant proteins.

1. Introduction

Human induced pluripotent stem cells (hiPSCs), reprogrammed from adult somatic cells, e.g., by using Yamanaka factors OCT4, SOX2, KLF4, and C-MYC (OSKM), have the unique ability to self-renew and differentiate into specialized cells in the human body.^[1] These merits make hiPSCs important for applications such as regenerative and transplant medicine,^[2] disease modeling,^[3] drug discovery, toxicological screenings,^[4] personalized medicine, and human developmental biology.^[5] To support self-renewal and growth of hiPSCs in vitro, hiPSCs were usually cultured on a feeder cell layer of mitotically inactivated mouse embryonic fibroblasts or immortalized embryonic fibroblast lines in culture medium with fetal calf serum or serum replacement.^[6] Currently, hiPSCs are cultured on a feeder-free but animal-derived basement membrane extract such as Matrigel™ (Corning Life Sciences, Corning,

Y. Liu, A. A. Popova, P. A. Levkin
Institute of Biological and Chemical Systems – Functional Molecular Systems
Karlsruhe Institute of Technology
Hermann-von-Helmholtz-Platz 1, 76344 Eggenstein-Leopoldshafen, Germany
E-mail: levkin@kit.edu
S. Bertels, M. Bastmeyer
Zoological Institute
Cell- and Neurobiology
Karlsruhe Institute of Technology
Fritz-Haber-Weg 4, 76131 Karlsruhe, Germany

M. Reischl
Institute for Automation and Applied Informatics
Karlsruhe Institute of Technology
Hermann-von-Helmholtz-Platz 1, 76344 Eggenstein-Leopoldshafen, Germany
R. Peravali, M. Bastmeyer
Institute of Biological and Chemical Systems – Biological Information Processing
Karlsruhe Institute of Technology
Hermann-von-Helmholtz-Platz 1, 76344 Eggenstein-Leopoldshafen, Germany
P. A. Levkin
Institute of Organic Chemistry
Karlsruhe Institute of Technology
Kaiserstraße 12, 76131 Karlsruhe, Germany

 The ORCID identification number(s) for the author(s) of this article can be found under <https://doi.org/10.1002/adhm.202200718>

© 2022 The Authors. Advanced Healthcare Materials published by Wiley-VCH GmbH. This is an open access article under the terms of the Creative Commons Attribution-NonCommercial License, which permits use, distribution and reproduction in any medium, provided the original work is properly cited and is not used for commercial purposes.

DOI: 10.1002/adhm.202200718

NY, USA),^[7] Geltrex™ (ThermoFisher Scientific, Waltham, MA, USA),^[8] or Cultrex® (Trevigen, Gaithersburg, MD, USA).^[9] However, the applicability of these coatings for *in vitro* culture of hiPSCs is challenging because of their inherent mechanical and biochemical properties. For example, Matrigel gels at 22–37 °C, making it impossible to dispense or pipette at room temperature (RT). More importantly, it varies in its biochemical and mechanical properties within and between batches.^[10] Moreover, it contains animal-derived materials, which impedes the clinical application of hiPSCs in regenerative and transplant medicine. The utilization of functional stem cells or their targeted differentiation products in human body requires a clinically-grade production process to ensure the purity, reproducibility, and tissue specific differentiation of patient-specific hiPSCs to avoid immune rejection, as well as microbial and viral transfer.

Proteins of human origin used either as a coating or as an additive to the culture medium are more suited for hiPSC culture because of their chemically defined nature and human origin, which is essential for any clinical applications of hiPSCs. For the purpose of maintaining hiPSCs pluripotency, a stem cell niche requires not only growth factors, but also cell adhesion, where extracellular matrix (ECM) proteins and surface proteins play extremely important roles. ECM proteins and surface proteins could mediate cell-ECM interaction and cell-cell interaction, respectively, which are of importance for hiPSCs self-renewal and proliferation. Literature reports a few well-defined ECM proteins that provide artificial ECM-like microenvironments for feeder cell-free hiPSC culture by enhancing cell-matrix interactions. These proteins include laminin 511 and vitronectin.^[11] Cell-Cell interactions are also important in the process of self-renewal and proliferation of hiPSCs. For example, the surface protein E-cadherin facilitates expansion of human pluripotent stem cells (hPSCs) in the form of colonies,^[12] and epithelial cell adhesion molecule (EPCAM) is involved in maintaining the undifferentiated status of human embryonic stem cells (ESCs).^[13] These proteins are chemically defined, of human origin, biocompatible, biodegradable and commercially available, which makes them good candidates for studying their effect on hiPSCs. Furthermore, cells in any tissue of the human body are simultaneously exposed to multiple proteins – the combinations and concentrations of which are important for the cell homeostasis, viability, and differentiation. Thus, it is crucial to study the influence of both single human-derived proteins and their combinations on hiPSCs. The proteins that might play a role in the self-renewal and differentiation of human stem cells according to the literatures were picked to conduct the protein screening. Based on the price and commercial availability, 11 human originated proteins that could be potentially used by others were selected. However, since the production of human recombinant proteins is extremely costly,^[14] conventional high-throughput screenings (HTS) using non-miniaturized platforms become immensely expensive and unaffordable to regular biology labs. Thus, to enable a systematic study of human-derived protein coatings capable of controlling hiPSC pluripotency, we drew attention to the droplet microarray (DMA) platform – a new miniaturized HTS approach.

Several high-throughput array-based approaches have emerged as screening tools for the *in vitro* culture of hiPSCs.^[14b,15] Mei et al. reported an array of polymer blends to investigate how the wettability, surface topography, surface

chemistry, and indentation elastic modulus influence self-renewal of hPSCs.^[16] Celiz et al. utilized a high-throughput microarray screening platform to search for substrates suitable for expansion and multilineage differentiation of hPSCs,^[17] and identified poly(HPhMA-co-HEMA) as an ideal substrate for that purpose. In a different study using high-throughput protein microarrays, Ireland et al. identified three novel coatings leading to two fold higher proliferation rates and expression of OCT4, NANOG, and SOX2 in hPSCs compared to Geltrex™ and vitronectin coatings.^[18] Nevertheless, there is usually no physical separation between experimental spots, requiring full immersion of the array into the medium, which poses a risk of cross talk between individual experiments.^[16–18] Despite obvious progress in adopting miniaturized array-based approaches in studies of hiPSCs, most screenings are performed in the 96- or 384-well plates, which is associated with high and sometimes unbearable consumption of proteins and hiPSCs.

The DMA platform relies on the ability of hydrophilic spots surrounded by a superhydrophobic background to precisely position and confine sub-microliter droplets inside the hydrophilic regions. The advantage of the DMA over microtiter plates is that it does not rely on gravity or plastic walls to position and confine droplets and, thus, can operate with much smaller fluid volumes, typically 100 to 300 nL for 500 to 1000 μm diameter hydrophilic spots. The deposition of liquids is performed using conventional noncontact liquid dispensers. This approach has been used for diverse biological and chemical applications, including transfection enhancer screening,^[19] formation and screening of mouse embryoid bodies,^[20] screening of zebrafish embryo,^[21] controllable assembly of tumor spheroids,^[22] high-throughput synthesis of lipidoids and screening for their transfection efficiency,^[23] and miniaturized combinatorial synthesis followed by cell screening.^[24] The DMA platform is compatible with noncontact methods of dispensing cell suspension to form high-density nanoliter cell arrays. It has multiple advantages over other techniques. First, there is no cross-contamination between spots because liquids are confined within hydrophilic spots, and a noncontact dispensing method can be used. Second, the use of nanoliter volumes significantly reduces the overall costs of expensive reagents and cells. DMA slides with 672 individual spots (**Figure 1**) require ≈8.3 μg of protein, ≈2.8 × 10⁵ cells and ≈0.28 mL of cell culture media to screen 231 protein combinations (single, binary, and ternary combinations). ≈866-fold and 25-fold less protein and cells than that is needed to perform the same screen in the 96-well plate format. In addition, miniaturization and high throughput allows for multiple experiment replicates to be introduced, thereby reducing variability.

In the current study, we employed a DMA-based HTS approach to investigate the influence of 231 protein combinations (11 proteins, 55 binary, and 165 ternary combinations) on the maintenance of pluripotency of hiPSCs. For this study we selected 11 proteins (**Table 1**) including Thy-1, ephrin type-B receptor 4 (EphB4), ephrin type-A receptor 1 (EphA1), E-cadherin, coxsackie and adenovirus receptor (CAR), junctional adhesion molecule A (JAM1), EPCAM, basigin (BSG), dystroglycan (DAG1), hyaluronic acid (HA), and laminin 521 (LN521). EphB4 belongs to Eph receptor tyrosine kinase, which promiscuously binds transmembrane ephrin-B family ligands residing on adjacent cells and mediates cell-cell interactions.^[25] EphB4

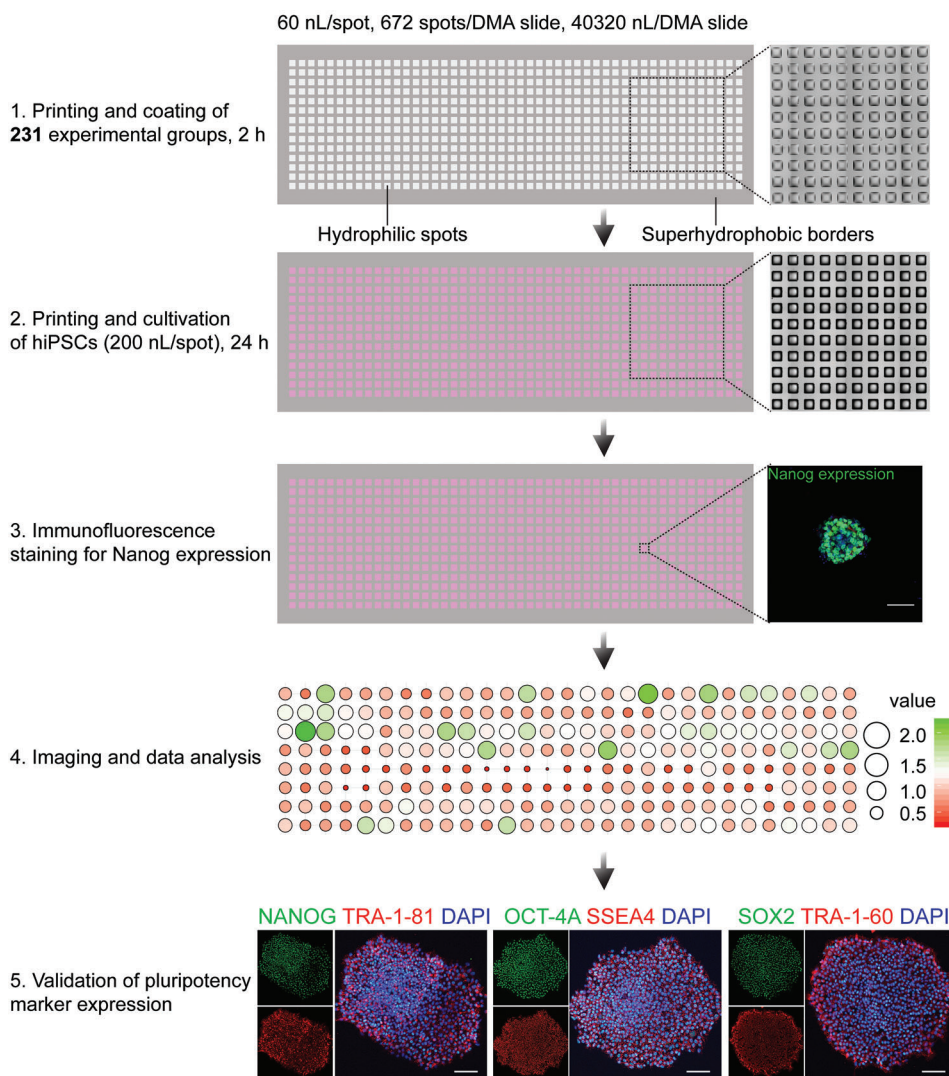
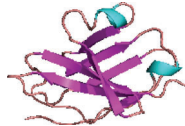
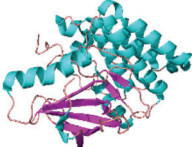

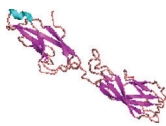
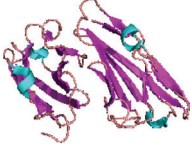
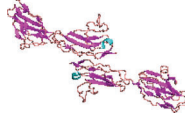
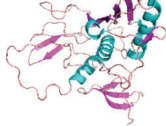
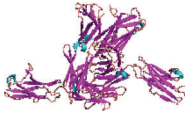
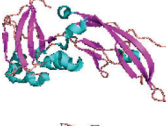



Figure 1. Schematic representation of the screening workflow. Printing: 60 nL of protein solution (final concentration of each protein of $10 \mu\text{g mL}^{-1}$) was printed onto each pre-determined spot and incubated at RT for 2 h, followed by adding cell suspension. Cultivation: hiPSCs were dispensed in a volume of 200 nL per spot and the array was cultured for 24 h before IF staining for measuring the NANOG expression. Image analysis: mean fluorescence intensity of IF staining was quantified. The size and color of the circles correspond to the relative expression of NANOG as measured by immunofluorescence: the lower left corner corresponds to the expression of Matrigel control, red and small size indicate lower expression than that of Matrigel control, while green color and large circles indicate expression of NANOG higher than that of Matrigel. The primary HTS was done with 11 single proteins, 55 binary combinations, and 165 ternary combinations, a total of 231 screening groups. Validation: hits were selected and further validated in hiPSCs by immunofluorescence staining of a larger set of pluripotency markers (Transcription factors: NANOG, SOX2, OCT-4A, cell surface markers: SSEA4, TRA-1-81, and TRA-1-60) and during a five weeks long culture period. Scale bar: 50 μm .

contributes to tumor malignancy and regulates the development of various tumors. EphB4 can also promote the self-renewal and proliferation of human neural stem cells. However, little is known about the role of EphB4 in the maintenance of pluripotency in hiPSCs. As for EphB2, a literature search could not find any direct evidence that EphB2 is expressed by undifferentiated hiPSCs.^[26] Miura et al. reported that EphB2 is a target protein of Wnt enriched in Lgr5⁺ intestinal stem cells. Leung et al. showed that the high expression of EphB2 enhanced cancer stem cell properties in hepatocellular carcinoma.^[27] Thus, we would speculate that EphB2 might play a role in hiPSCs via Wnt signaling pathway. However, further investigation and vali-

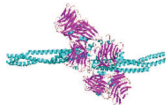
dation are needed. DAG1 is a heavily glycosylated protein that is strongly expressed on/by hiPSCs.^[28] It can interact not only with laminin to mediate cell–ECM interactions, but also participates in direct signaling events, together with integrins. EpCAM is a transmembrane glycoprotein, which mediates cell–cell interactions via cadherins linking the cytoskeleton. It is a pluripotency-related gene in induced pluripotent stem cells.^[29] BSG is a member of the immunoglobulin superfamily, which is involved in reproduction, neural function, inflammation, and tumor invasion. It is a cell surface marker that is consistently upregulated in early and late passages of hiPSCs.^[30] Laminins (LNs) are well-known ECM proteins, which contribute to ECM structure and have ef-

Table 1. Proteins used in this study with their corresponding structures and Protein Data Bank (PDB) codes.

Protein	Description	Structure	PDB code
Thy-1 (CD90)	Glycophosphatidylinositol (GPI) anchored conserved cell surface protein, combinatorial surface marker for stem cells		Modeling by SWISS-MODEL with ProMod3 3.0.0
Ephrin type-B receptor 4 (EphB4)	Membrane-bound protein, binding and activation of Eph/ephrin intracellular signaling pathways, involved in the regulation of cell adhesion and migration		6fnn ^[43]
Ephrin type-A receptor 1 (EphA1)	Membrane-bound protein, binding and activation of Eph/ephrin intracellular signaling pathways, regulates cell proliferation		3kka
E-cadherin	Calcium-dependent cell–cell adhesion glycoprotein comprising five extracellular cadherin repeats, a transmembrane region, and a highly conserved cytoplasmic tail		2O72 ^[34]
Coxsackie and adenovirus receptor (CAR)	Transmembrane bound protein with two immunoglobulin (Ig)-like extracellular domains, a transmembrane domain, a cytoplasmic domain, and two N-linked glycosylation sites, may function as a cell adhesion molecule		1f5w ^[35]
Junctional adhesion molecule A (JAM-A, JAM-1 or f11r)	Junctional adhesion molecule transmembrane protein family member, receptor of chimeric antigen receptor (CAR)		1nbq ^[36]
Epithelial cell adhesion molecule (EpCAM)	Transmembrane glycoprotein involved in cell signaling, migration, proliferation and differentiation, involved in embryonic stem cell proliferation and differentiation		4mzv ^[37]
Basigin (BSG or CD147)	Member of the immunoglobulin superfamily, fundamental in intercellular recognition, involved in various immunologic phenomena, differentiation, and development		3b5h ^[38]
Dystroglycan (DAG1)	Transmembrane linkage between the extracellular matrix and the cytoskeleton, involved in several processes, including laminin and basement membrane assembly		5llk ^[39]
Hyaluronic acid (HA)	Chief component of the extracellular matrix, contributes to cell proliferation and migration		1poz ^[40]

(Continued)

Table 1. Continued.

Protein	Description	Structure	PDB code
Laminin 521	A component of the extracellular matrix, used to enhance pluripotent stem cell culture		5xau ^[41]

Helix

Sheet

Loop

fects on cell adhesion, differentiation, migration, and other cell behaviors.^[31] α -5 LN promotes the self-renewal of hiPSCs.^[32] However, to the best of our knowledge, the roles of these proteins in the undifferentiated culture of hiPSCs and their impact on maintaining pluripotency of hiPSCs have not been investigated yet. Other important reasons for the selection of the 11 proteins were their commercial availability and reasonable price, which is important to make sure that the identified protein coatings could find broad application in the scientific community.

The printing parameters were investigated and optimized to achieve a high cell survival rate in nanoliter droplets on DMA. The pluripotency of hiPSCs on DMA was monitored by immunofluorescence (IF) staining of NANOG. Ten protein combinations were found to maintain the pluripotency of hiPSCs. Of these, two most effective protein combinations BIK (EphB4 + DAG1 + LN 521) and GHK (EpCAM + BSG +LN 521) were further validated by long-term culture of hiPSCs, and by investigating their ability to differentiate into the three germ layers. The proteins and protein combinations identified in this study can be used as chemically defined and xeno-free substrates for hiPSC culture, which holds great potential for clinical and biomedical applications.

2. Results and Discussion

2.1. Cost-Effective DMA-Screening to Identify Xeno-Free hiPSC Culture Conditions

The layout of a DMA slide and the workflow for screening proteins are described in Figure 1. The DMA is a 2.5 × 7.5 cm glass slide with a 14 × 48 array of hydrophilic spots with superhydrophobic (SH) borders, resulting in 672 independent 1 × 1 mm square spots separated by 500 μ m SH borders. For this study we selected eleven single proteins (Table 1) as well as their binary and ternary combinations – in total 231 experimental groups. In order to study their synergistic effects, additional 55 binary and 165 ternary combinations were tested (Table S1, Supporting Information). To create protein arrays, the individual protein solutions (60 nL with 10 μ g mL⁻¹ in protein dilution buffer) were dispensed onto individual 1 mm × 1 mm spots of the DMA using a noncontact liquid dispenser (Figure S1A, Supporting Information). To reduce experimental error, each protein or combination was printed in six replicates, demonstrating the advantage of miniaturization that enables the fabrication of a high-density array. Then, 200 nL of suspension of hiPSCs were printed per spot, followed by culturing on DMA slides for 24 h (Figure S1B, Supporting Information). Cells were then stained for NANOG

(an indicator of pluripotency) by IF staining, followed by automated imaging.^[42] The primary screen was used to identify hits on the basis of their ability to maintain pluripotency compared to Matrigel, which was used as a positive control. Selected hits were then validated for their ability to maintain the expression of several pluripotency markers, including NANOG, TRA-1-81, OCT-4A, SSEA4, SOX2, and TRA-1-60 in a 5 weeks long culture. Finally, the ability of cultured cells to differentiate into three germ layers (ectoderm, mesoderm, and endoderm) was tested.

HiPSCs are very sensitive to environmental stimuli, such as compression and shearing forces. They are also prone to cell death after dissociation during regular expansion,^[43] which makes HTS of hiPSCs especially challenging since manual removal of differentiated cells as well as dead cells from undifferentiated live cells is not possible in screening experiments. Therefore, we first compared the viability of hiPSCs cultured on DMA in 200 nL using either manual seeding (58.28 ± 1.90%) or after noncontact cell printing (69.43 ± 5.90%) after 24 h culture (Figure S2, Supporting Information). The viability was measured by a live–dead staining as described previously.^[44] The viability of cells after noncontact printing was higher than that of manual seeding. This might be due to the higher volume of each spot after printing (200 nL) than the volume of manual seeding (\approx 80 nL) could provide more nutrient for cell growing and survival. Thus, we selected noncontact printing for the further experiments.

Using IF staining for the pluripotency markers SOX2, OCT-4A, NANOG, TRA-1-60, SSEA4, and TRA-1-81, we next assessed whether the Matrigel-coated DMA could maintain the pluripotency of hiPSCs. Typical IF staining procedures involve washing steps, which often result in cell loss. Thus, we assessed the changes in cell numbers before and after IF staining. As shown in Figure S3 (Supporting Information), 50% of hiPSCs were left in DMA spots after IF staining. Average numbers of hiPSC colonies after IF staining were also investigated; there were approximately seven colonies in one DMA spot, with no significant difference between colony numbers remaining among three biological repeats (Figure S4, Supporting Information). These results indicated the feasibility and reproducibility of the established protocol for IF staining on DMA. IF staining results (Figure 2A) indicated that expression of pluripotency markers in hiPSCs grown on DMAs was similar to that in cells cultured in multi-well plates (Figure S5, Supporting Information), demonstrating that hiPSCs cultured on DMAs retained their pluripotency and ability to self-renew. Next, we used phalloidin staining to visualize the typical cytoskeletal arrangement of hiPSCs colonies; for hiPSCs cultured on DMAs, well assembled and organized F-actin cytoskeletal

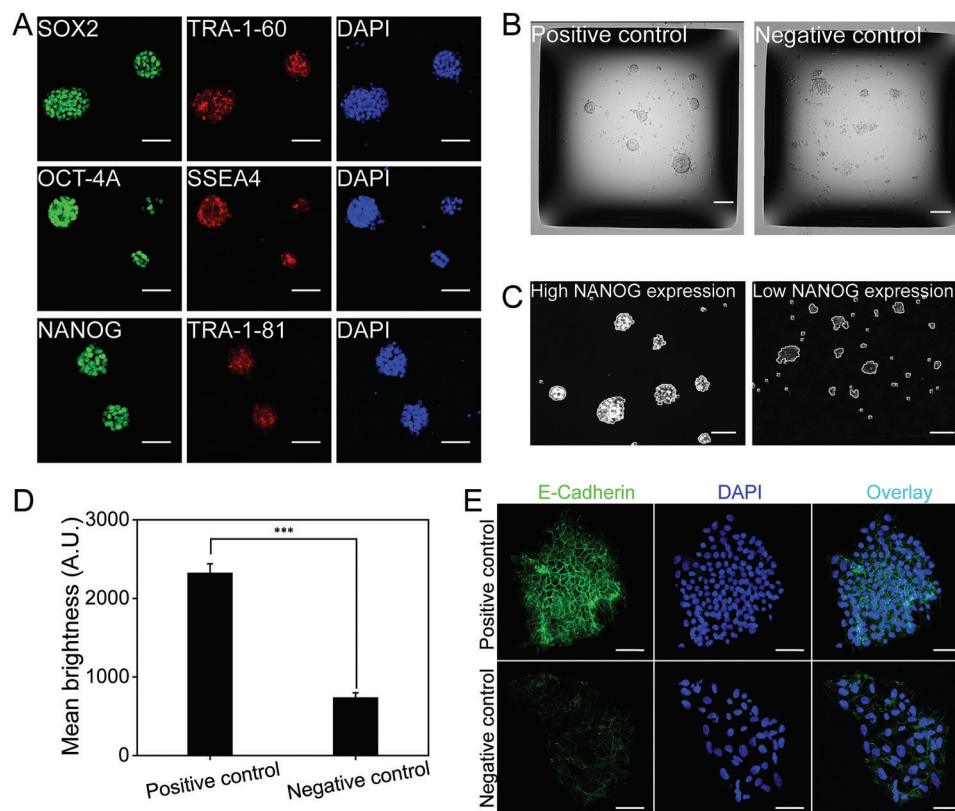


Figure 2. Validation of the screening protocol. A) Representative confocal laser scanning microscope (CLSM) images of hiPSCs cultivated in 200 nL droplets on DMA slides coated with Matrigel and stained for six pluripotency markers: SOX2, OCT-4A, NANOG, TRA-1-60, SSEA4, and TRA-1-81. Three independent experiments ($n = 3$) obtained comparable results. DAPI was used to counterstain nuclei. Scale bars: 50 μm . B) Bright-field images of hiPSCs cultivated on positive (Matrigel, MG^+) and negative (no Matrigel, MG^-) controls. Scale bar: 100 μm . C) NANOG expression level was used as a read out for the primary screening. IF staining was carried out on DMA followed by automated microscopy. All colonies in one image were from the single droplet. Scale bar: 50 μm . D) Quantification of mean brightness (mean fluorescence intensity) of hiPSCs cultured on positive and negative controls and stained for the pluripotency marker NANOG. The mean fluorescence intensity was calculated as the total fluorescence intensity divided by the area (in pixels). $***p < 0.001$, significant differences positive control and negative controls. (Z' value is between 0.5 and 1, corresponding to a high-quality screening assay). Data were presented as mean \pm 3SD. ($n = 3$) E) Representative CLSM images of E-cadherin expression in hiPSCs cultured on positive and negative control coatings. E-cadherin mediates cell–cell interactions and contributes to stem cell colony formation and pluripotency. Thus, on the positive control coating, undifferentiated hiPSCs show high expression of E-cadherin, while differentiated hiPSCs on the negative control coating show low-to-no E-cadherin expression. DAPI was used to counterstain nuclei. Scale bar: 25 μm .

organization was observed (Figure S6, Supporting Information), indicating the feasibility of using DMA for hiPSCs cultivation.

Taken together, our results demonstrated that hiPSCs cultured in 200 nL droplets on the DMAs show the same characteristics (expression of pluripotency markers) as cells cultured in a microtiter plate. This opens the possibility to use the DMA platform for culturing and screening undifferentiated hiPSCs.

As a next step, the robustness of utilizing the DMA platform for HTS of hiPSCs was assessed. Matrigel coating (MG^+) was set as a positive control and no Matrigel coating (MG^-) was set as a negative control. The morphology of hiPSCs in positive and negative controls are shown in Figure 2B. The positive control group demonstrated typical hiPSC morphology, with compacted cells and distinct edges. In the negative control group, hiPSCs displayed poor aggregation with no distinct edges and compacted cells.

NANOG, OCT4, and SOX2 are the core transcription factors regulating pluripotency of stem cells. While the expression of

OCT4 and SOX2 is relatively uniform, stem cells fluctuate between high NANOG expression with high pluripotency and low NANOG expression with low pluripotency.^[45] Hence, NANOG expression detected by IF staining was selected to be the read-out for the primary screening, i.e., higher mean fluorescence intensity of cells should indicate higher self-renewal (Figure 2C,D), which was confirmed by a significant difference in mean fluorescence intensity for NANOG expression in positive and negative controls (Figure 2D).

We then used the screening window coefficient, Z-factor (Z'), to evaluate the quality of our primary HTS assay.^[46] Z' was calculated from three biological replicates using the formula:

$$Z' = 1 - \frac{(3\sigma_{c+} + 3\sigma_{c-})}{|\mu_{c+} - \mu_{c-}|} \quad (1)$$

in which σ_{c+} is the standard deviation (SD) of the positive control, σ_{c-} represents the SD of the negative control, μ_{c+} and μ_{c-} are the

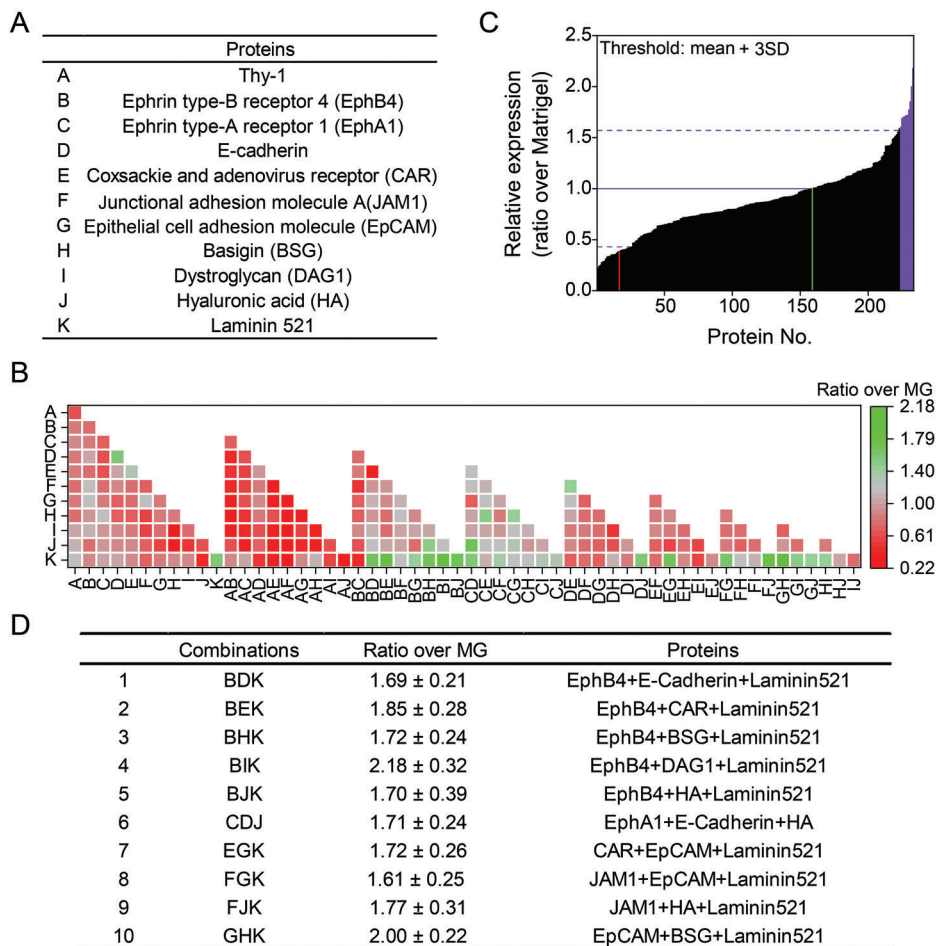


Figure 3. Results of the primary protein screening. A) List of proteins and their corresponding letter codes used in the screening. B) Heat map showing the fold change of NANOG expression in hiPSCs cultured on coatings containing single proteins and protein combinations. Six replicates were used for each independent array experiment. The mean fluorescence intensity of NANOG expression of each independent group was normalized against expression level of NANOG in cells cultured on Matrigel (MG) coating (positive control). Green indicates high NANOG expression level (higher capacity for self-renewal) and red indicates low NANOG expression (lower capacity for self-renewal) than marker expression levels in cells cultured on a positive control (MG⁺) coating. C) Graph showing relative NANOG expression of all tested protein groups in the screening. The threshold for protein coating promoting significant change in NANOG expression was set as mean + 3 SD. Red column indicates negative control (non-coated, MG⁻), green column indicates positive control (MG-coated, MG⁺), and violet columns show positive hits. D) The list of top ten positive hits identified in the primary screening.

means of fluorescence intensity of positive and negative control, respectively. The value of Z' was 0.64 (Figure 2D), confirming the high quality of the assay.^[46]

Along with various transcription factors, E-cadherin is important for establishing and maintaining stem cell pluripotency and their ability to self-renew via cell–cell adhesions.^[47] Therefore, we investigated E-cadherin expression in hiPSCs in both the positive and negative controls (Figure 2E). High E-cadherin expression was observed in positive controls, while low-to-no E-cadherin expression was observed in negative controls. The mean E-cadherin fluorescence intensity of negative controls was $17.01 \pm 7.84\%$ of that of positive controls (Figure S7, Supporting Information). The results demonstrated the significant difference of E-cadherin expression between positive and negative control, indicating the high quality of the HTS assay and the robustness of utilizing the DMA platform for HTS of hiPSCs.

2.2. Specific Ternary Protein Combinations Promote Pluripotency Marker Expression

For the primary screening, hiPSCs were cultured on coatings created from 231 protein groups (11 single proteins (Figure 3A), 55 binary combinations of these proteins, and 165 ternary combinations of these proteins). The proteins were stored as lyophilized powder with determined weight at -80°C before use. In order to coat surfaces with different protein combinations, we deposited 60 nL of $10 \mu\text{g mL}^{-1}$ solution of each protein in a protein dilution buffer into 1 mm square hydrophilic spots on DMA slide, followed by incubation of the droplet array at 25°C in a sealed petri dish on the clean bench for 2 h. Cells were then seeded by printing 200 nL of cell suspension into each spot. The DMA slide was then placed in the cell incubator for 24 h, followed by IF staining for NANOG and imaging.

Table 2. Comparison of reagent use, cell consumption, and estimated cost for the screening of 231 protein combinations performed on DMA with hypothetical identical screenings utilizing 384- or 96-well plates. Six replicates for each experimental group were calculated. The volumes of individual experiments in DMA, 384- and 96-well plates used for the calculation are 200 nL, 10, and 50 μ L, respectively.

Parameter	DMA	384-well plates	96-well plates
Volume of protein solutions (mL)	≈ 0.08	≈ 13.9	≈ 69.3
Amounts of proteins (μ g)	≈ 0.8	≈ 139	≈ 693
Number of cells	$\approx 2.8 \times 10^5$	$\approx 3.1 \times 10^6$	$\approx 6.9 \times 10^6$
Volume of medium (mL)	≈ 0.28	≈ 27.7	≈ 231.6
Estimated costs of used proteins (\$)	≈ 170	≈ 4000	≈ 14300

In total, only 83 μ L of protein solution (0.83 μ g protein), $\approx 2.8 \times 10^5$ cells, and ≈ 0.28 mL of cell culture medium was required for the whole primary screening using 4 DMA slides. This decreased the consumption of proteins and cell suspension by 860- and 25-fold, respectively, if the HTS had to be conducted in conventional 96-well plates, demonstrating the potential and importance of miniaturization, especially, when working with such expensive substances as proteins (Table 2). The mean fluorescence intensity representing NANOG expression level in hiPSCs cultured on each protein coating was then analyzed and normalized against the intensity of cells cultured on positive control coatings (MG⁺ spots). Figure 3B presents a schematic of the protein combinations used in the experiment (A–K), and a heat map representing the ratio of NANOG expression of hiPSCs grown on different experimental protein groups versus cells grown on a positive control coating. In the heat map, red indicates lower NANOG expression (cell differentiation) and green represents higher NANOG expression (cell self-renewal) compared with its expression level in cells cultured on the positive control coating (MG⁺). The threshold of mean + 3 SD (1.00 + 0.57) compared with positive control (MG⁺) was established to identify positive hits showing significantly increased NANOG expression in hiPSCs.^[48] The ten top protein groups were identified (Figure 3C,D; a detailed description of these is presented in Figure S8, Supporting Information). In Figure 3C, the green, red, and violet columns indicate relative NANOG expression level in hiPSCs cultured on positive (MG⁺) and negative (MG⁻) control coatings, and hits in the primary screening, respectively. The fold changes of experimental groups versus MG ranged from 0.22 (red) to 2.18 (green). Two protein groups that promoted the strongest increase in NANOG expression in hiPSCs were BIK (EphB4 + DAG1 + LN 521) and GHK (EpCAM + BSG + LN 521), with 2.18 ± 0.32 and 2.00 ± 0.22 -fold increase, respectively (Figure 3B,D).

The results of our primary screening showed that single proteins did not promote NANOG expression in hiPSCs compared to MG coating. However, protein combinations, particularly protein ternary groups, resulted in significantly higher expression of pluripotency markers in hiPSCs compared to cells cultured on the MG coating (Figure 3D). LN 511 coating has been reported to support the long-term self-renewal of human pluripotent stem cells.^[49] Another study demonstrated that LN 521 in combination with fibronectin could support the greatest cell attachment.^[18] Furthermore, LN 521/E-cadherin matrix could support the clonal culture of human stem cells.^[50] From our screening results, LN

521 alone showed the ability to maintain the pluripotency of hiPSCs (high NANOG expression when compared with Matrigel group, Figure 3B; Figure S8, Supporting Information). However, the normalized value of LN 521 was less than the threshold value. Thus, LN 521 was not identified as “positive hit” in the screening.

2.3. Xeno-Free Substrates Maintain Differentiation Capacity During Long-Term Culture

To check whether all three selected GHK proteins were present on the surface after the coating procedure, we performed IF staining following the surface coating. GHK proteins were coated onto 96-well plates at RT for 2 h, then the solution was aspirated and the plates were washed with PBS for three times. The IF staining was conducted as follows, the coated plates were incubated with 1% BSA, primary antibodies (anti-BSG, anti-EpCAM and anti-Laminin alpha 5), and secondary antibodies before imaging. As can be seen in Figure S9 (Supporting Information), there was no autofluorescence background from the IF staining procedure and the plates (groups “no primary” and “no secondary”). The fluorescence staining from images confirmed that the proteins were successfully coated on the plate (Figure S9, Supporting Information).

To identify the most effective proteins for the maintenance of pluripotency of hiPSCs in long-term in vitro culture and also to validate the discovered hits as a coating of regular polystyrene plates, two most effective positive protein combinations (BIK and GHK) and one negative protein combination (DIK: E-Cadherin+DAG1+LN 521) were selected for further validation in 12-well plates. DIK was selected because of its ability to induce cell attachment, while at the same time leading to a reduced NANOG expression compared to the positive control and because it also contains LN 521 (K), which was present in both top hits. Thus, inability of the DIK to maintain pluripotency would confirm that combination of the proteins and not LN 521 itself is responsible for the observed effect. DIK (E-Cadherin+DAG1+LN 521), BIK (EphB4 + DAG1 + LN 521), and GHK (EpCAM + BSG + LN 521) were coated onto 12-well plates at RT for 2 h, then the solution was aspirated before adding hiPSCs. These two positive protein combinations could facilitate attachment of hiPSCs in in vitro culture for up to 4 days – similar to MG (Figure 4A). On day 1, compared with MG (set as 100%), the attachment efficiencies of DIK (E-Cadherin, DAG1, LN 521), BIK (EphB4 + DAG1 + LN 521), and GHK (EpCAM + BSG + LN 521) were $91.86 \pm 3.90\%$, $94.76 \pm 3.44\%$, and $95.84 \pm 9.78\%$, respectively. The attachment efficiency of DIK was $88.00 \pm 4.77\%$ for day 2, $85.46 \pm 10.02\%$ for day 3, and $74.38 \pm 5.36\%$ for day 4. Over the following three days, BIK showed high attachment efficiency for day 2 ($92.59 \pm 6.00\%$), day 3 ($84.15 \pm 9.16\%$), and day 4 ($79.13 \pm 12.57\%$). GHK showed similar attachment efficiency for day 2 ($91.14 \pm 12.67\%$), day 3 ($79.81 \pm 6.84\%$), and day 4 ($78.48 \pm 1.91\%$). On the contrary, hiPSCs completely failed to attach on non-coated well plates. These results demonstrate that DIK, BIK, and GHK can facilitate the attachment of hiPSCs in culture to a similar extent as Matrigel. These three protein groups all contain LN 521 (K), which implies the cell attachment could be facilitated by LN 521 through interaction with $\alpha 6\beta 1$ integrin.^[50] Over five passages, hiPSCs cultured on BIK and GHK displayed both typical hiPSC colony morphol-

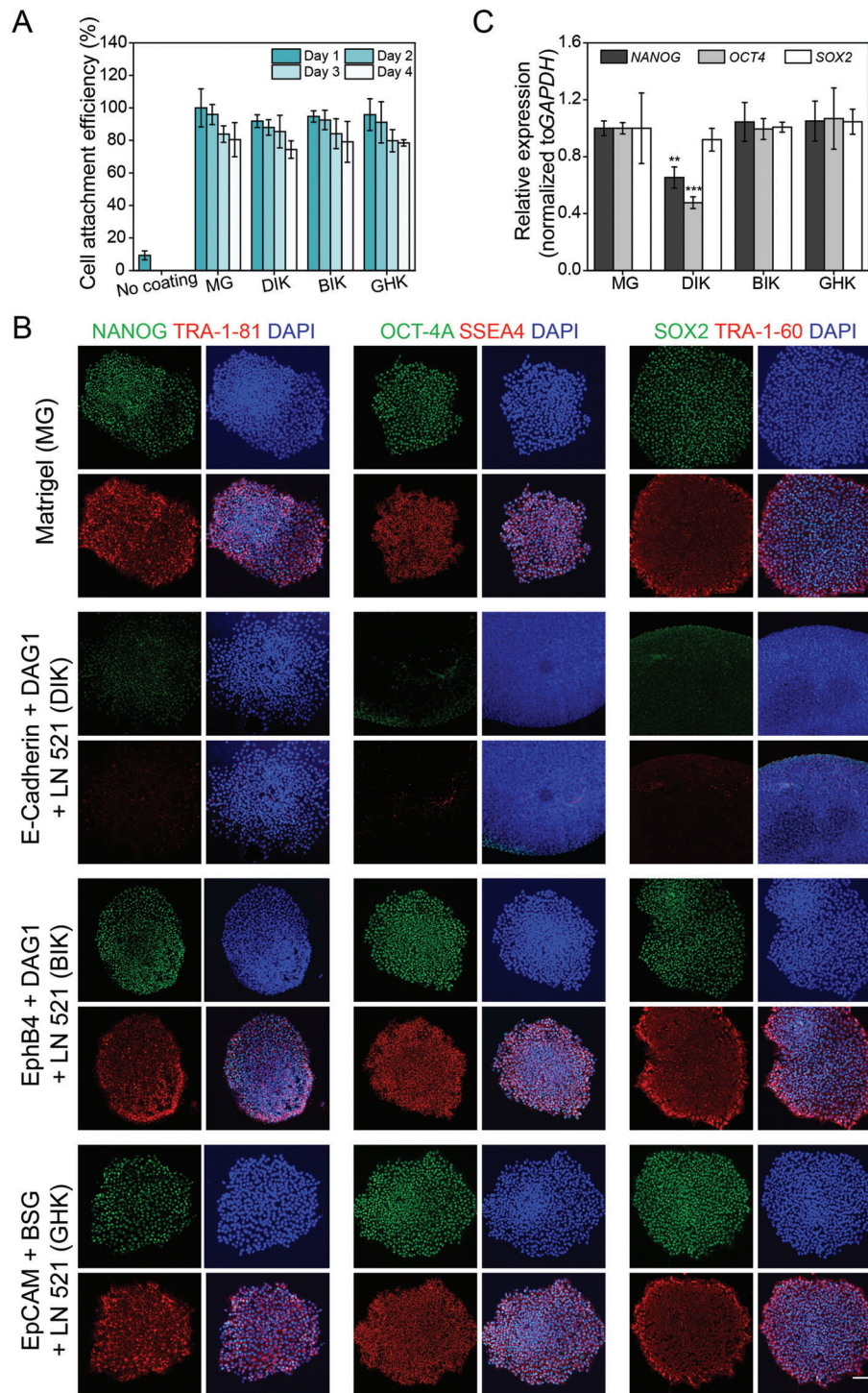


Figure 4. Effect of protein coatings on hiPSC's long-term culture: validation of the efficiency of two most effective ternary protein combinations (BIK and GHK). A) Colony attachment efficiency of hiPSCs on non-coated 12-well plates, Matrigel (MG)-coated 12-well plates, and DIK, BIK, and GHK-coated 12-well plates for 4 days. BIK (EphB4 + DAG1 + LN 521), and GHK (EpCAM + BSG + LN 521) were identified from the primary screening as showing stronger NANOG expression, while cells cultured on DIK (E-Cadherin + DAG1 + LN 521) protein group showed lower NANOG expression. Data were presented as mean \pm 3SD. ($n = 3$) B) IF images of hiPSCs cultured on MG, DIK, BIK, and GHK coatings and stained for six pluripotency markers: NANOG, OCT-4A, SOX2 (green fluorescence); TRA-1-81, SSEA4, TRA-1-60 (red fluorescence). Scale bar: 50 μ m. C) qPCR profiling of pluripotency marker genes (NANOG, OCT4, and SOX2) of hiPSCs grown on MG, DIK, BIK, and GHK-coated well plates for five passages ($n = 3$, biological replicates). Gene expression data were normalized against a reference gene *GAPDH*. In hiPSCs cultured on DIK, BIK, and GHK coatings, the gene expression level was normalized against that of cells grown on MG. Data are represented as mean \pm SEM. $**P < 0.01$ and $***P < 0.001$, significant differences between MG and DIK groups.

ogy (Figure S10, Supporting Information) and levels of pluripotency marker (NANOG and TRA-1-81) expression comparable to that of cells cultured on Matrigel coating (Figures S11–S13, Supporting Information). However, cells cultured on DIK protein group gradually lost the expression of the pluripotency markers NANOG and TRA-1-81 (Figure S14, Supporting Information). This confirms that laminin is not enough to maintain pluripotency of hiPSCs despite efficient cell attachment.

To further validate the pluripotency of hiPSCs grown on DIK (E-Cadherin + DAG1 + LN 521), BIK (EphB4 + DAG1 + LN 521), and GHK (EpCAM + BSG + LN 521) coatings, the expression of pluripotency markers was investigated by IF staining and quantitative PCR (qPCR) analysis over five passages. HiPSCs cultured on BIK and GHK-coated surfaces stained positive for NANOG, OCT-4A, SOX2, TRA-1-81, SSEA4, and TRA-1-60, similar to cells cultured on Matrigel (Figure 4B; Figure S15, Supporting Information). HiPSCs cultured on DIK-coated surface showed a significantly lower expression for NANOG, OCT-4A, SOX2, TRA-1-81, SSEA4, and TRA-1-60, when compared to cells cultured on Matrigel. This demonstrates that, like Matrigel, BIK and GHK coatings can also support the long-term expansion of hiPSCs and inhibit differentiation of the hiPSCs. Even though DIK coating could facilitate the attachment of hiPSCs in culture for a long-term, it could not maintain the pluripotency of hiPSCs. These results confirm the relevance and robustness of the primary screening conducted using the DMA platform. The hiPSCs cultured on DIK (E-Cadherin + DAG1 + LN 521), BIK (EphB4 + DAG1 + LN 521), and GHK (EpCAM + BSG + LN 521) for 24 h showed different expression of NANOG in the primary screening, while the similar difference could also be observed in long-term and large-scale culture. These results also demonstrate that the presence of LN 521 alone in the ternary combination of proteins is not enough for maintaining the pluripotency of hiPSCs and only ternary protein combinations could lead to the efficient support of undifferentiated culture of hiPSCs.

To investigate the pluripotency marker expression at the gene level, qPCR analysis for NANOG, OCT4, and SOX2 was conducted. The gene expression of target pluripotency genes (NANOG, OCT4, and SOX2) was normalized against the expression level of glyceraldehyde 3-phosphate dehydrogenase (GAPDH), and expression levels of pluripotency genes in hiPSCs cultured on DIK, BIK, and GHK coatings were further normalized against expression levels of these genes in cells grown on Matrigel (Figure 4C). In hiPSCs cultured on Matrigel, DIK, BIK, and GHK coatings, gene expression levels of NANOG, OCT4, and SOX2 were 1.00 ± 0.05 , 1.00 ± 0.04 , 1.00 ± 0.25 ; 0.65 ± 0.07 , 0.48 ± 0.04 , 0.92 ± 0.08 ; 1.04 ± 0.14 , 0.99 ± 0.07 , 1.01 ± 0.03 ; and 1.05 ± 0.14 , 1.07 ± 0.22 , and 1.05 ± 0.09 , respectively (Figure 4C). The qPCR results demonstrated that hiPSCs cultured on BIK and GHK-coated surfaces expressed pluripotency marker genes at similar levels to those in cells cultured on Matrigel, while cells cultured on DIK-coated surface expressed lower pluripotency marker gene than cells cultured on Matrigel. Taken together, our results demonstrated that hiPSCs grown on BIK and GHK coated surfaces sufficiently support self-renewal and pluripotency of hiPSCs in feeder-free conditions, while DIK coated surface is not sufficient to support the pluripotency of hiPSCs. Comparing the results of BIK and DIK, the EphB4 (B) protein showed effectiveness in maintaining pluripotency of hiPSCs

while E-cadherin (D) was not efficient in maintaining pluripotency of hiPSCs when mixed with other proteins. This might be due to the interactions among the three proteins and/or the need for multiple protein-cell interactions combined with the required cell-surface adhesion. The results further confirm that not all ternary protein combinations work for maintaining the pluripotency of hiPSCs even though the cells can attach on the surface. Nevertheless, the results show that cell attachment is the essential step for maintaining pluripotency of hiPSCs. Different cells have distinct intrinsic characteristics. Using good manufacturing practice-compliant protocols to generate hiPSC lines plays an important role in the applied research of hiPSCs. Thus, the applicability of the protein combinations on other cell lines should be evaluated in the future.

A unique characteristic of hiPSCs is their ability to form an embryoid body (EB) and differentiate into three germ layers (pluripotency). Therefore, for cells cultured in vitro on BIK (EphB4 + DAG1 + LN 521) and GHK (EpCAM + BSG + LN 521)-coated surfaces, we investigated EB formation and the differentiation into three germ layers, according to a previously described method (Figure 5A).^[51] Briefly, hiPSCs grown on BIK and GHK-coated surfaces were dissociated after five passages and seeded in 25 μ L hanging droplets on the lid of a Petri dish. Two days later, EBs were transferred onto gelatin-coated coverslips in 12-well plates, followed by culturing for 14 days to induce spontaneous differentiation into three germ layers (endoderm, mesoderm, and ectoderm). Then, the samples were stained for specific germ layer markers (endoderm, FOXA2; mesoderm, brachyury; and ectoderm, β -Tubulin3). Cells originated from hiPSCs cultured on BIK and GHK-coated surfaces showed similar expression of three germ layer markers as cells obtained from Matrigel-coated surfaces (Figure 5B Figure S16, Supporting Information). Cells cultured on non-coated surface did not express markers of the three germ layers. These results demonstrate that BIK and GHK coatings are sufficient and effective in maintaining pluripotency and the differentiation capacity of hiPSCs, as confirmed by estimating cell attachment, expression of pluripotency markers (NANOG, OCT4, and SOX2) in long-term culture over five passages, formation of EBs, and differentiation into three germ layers.

3. Conclusion

In this work, we performed a high-throughput screening of 231 well-defined protein combinations, including 11 proteins, their 55 binary and 165 ternary combinations, using a miniaturized DMA platform. In this screening, we studied the influence of the protein combinations on the maintenance of pluripotency of hiPSCs cultured in individual 200 nL droplets. The primary screening revealed ten ternary protein combinations that could maintain the pluripotency of hiPSCs and resulted in a significantly stronger NANOG expression as compared to Matrigel. The long-term (5 weeks) maintenance of pluripotency of hiPSCs and their subsequent differentiation into three germ layers was also demonstrated, further proving the applicability of the identified novel protein combinations for xeno-free culture of hiPSCs. However, we would like to emphasize that one needs to determine the effects of the identified protein mixtures on cell growth and genomic stability prior to using them for hPSC expansion.

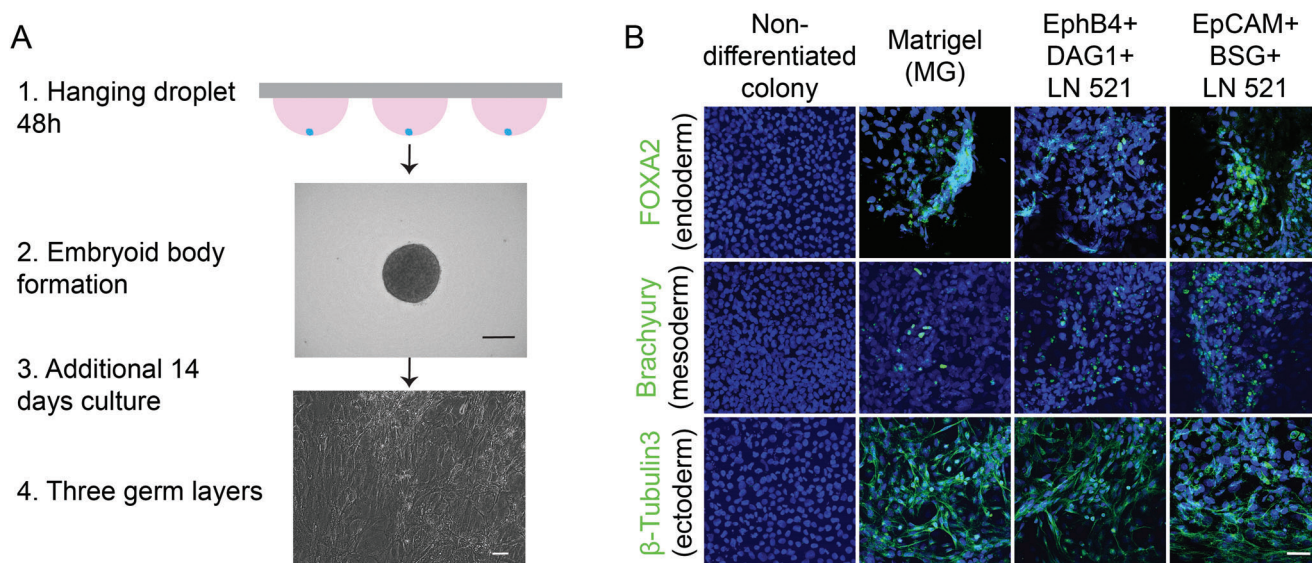


Figure 5. Validation of two hits from the primary screening by differentiation into three germ layers. A) Schematic diagram of the differentiation of hiPSCs into three germ layers. B) IF staining for markers of three germ layers FOXA2 (endoderm), brachyury (mesoderm), and β -Tubulin3 (ectoderm) in hiPSCs cultured on non-differentiated colony (NC), and surfaces coated with MG, BIK (EphB4 + DAG1 + LN 521), and GHK (EpCAM + BSG + LN 521). Scale bar: 20 μ m.

It is important to highlight that compared with HTS conducted in conventional 96-well plates, the primary HTS using the DMA platform required tremendously lower amounts of proteins and cells – only 83 μ L of protein solution (0.83 μ g total protein) and $\approx 2.8 \times 10^5$ cells, resulting in 866- and 25-fold decrease of consumption of proteins and cell suspension, respectively, and thus reducing the overall experimental costs. The newly discovered protein combinations are human originated and hold great potential for both fundamental and applied research using hiPSCs in various fields such as genetic disease models, drug discovery, and other biomedical applications. Finally, the HTS using the DMA platform demonstrates the great potential of this miniaturized technology for high-throughput studies of expensive but important small molecules, proteins or their combinations, and their influence on scarce and precious cell types, such as hiPSCs or human primary cells.

4. Experimental Section

Materials: Formaldehyde solution (16%), propidium iodide (PI, 1.0 mg mL⁻¹ in water), Calcein AM (1 mg mL⁻¹ in DMSO), 4', 6-diamidino-2-phenylindole (DAPI) were purchased from Thermo Fisher Scientific Inc. (MA, USA). Phosphate-buffered saline (PBS) was purchased from Gibco, Life Technologies GmbH (Darmstadt, Germany). Serum-free hiPSCs culture medium mTeSR™ plus, hiPSCs detaching reagent ReLeSR™, and Laminin 521 were purchased from STEMCELL technologies (Vancouver, Canada). Dulbecco's Modified Eagle Medium/F12 (DMEM/F12) was purchased from PAN Biotech (Aidenbach, Germany). Bovine serum albumin (BSA) was purchased from VWR international (Radnor, USA). Rabbit anti-OCT-4A, rabbit anti-SOX2, rabbit anti-NANOG, mouse anti-SSEA4, mouse anti-TRA-1-60(S), and mouse anti-TRA-1-81 antibodies were purchased from Cell signaling Technology (CST, Massachusetts, USA). Rabbit anti-E-cadherin, mouse anti-laminin alpha 5, Alexa Fluor® 405 goat anti rabbit IgG H&L, Alexa Fluor® 488 goat anti rabbit IgG H&L, Alexa Fluor® 488 rabbit anti goat IgG H&L, Alexa Fluor® 594 goat anti mouse IgG H&L antibodies,

and Hyaluronic acid sodium salt were purchased from Abcam (San Francisco, USA). LDEV-free Corning® Matrigel® hESC qualified Matrix was purchased from Corning (Massachusetts, USA). Doxycycline hyclate, Phalloidin-Atto 565, rabbit anti- β -Tubulin3 antibody, and Triton™ X-100 were purchased from Sigma-Aldrich (Steinheim, Germany). Normocin was purchased from InvivoGen (California, USA). Goat anti-brachyury, goat anti-human EpCAM, and goat anti-FOXA2 antibodies were purchased from R&D Systems (Minnesota, USA). Proteins (Thy-1, EphB4, EphA1, E-cadherin, coxackie and adenovirus receptor (CAR), JAM1, EpCAM, basigin (BSG), and dystroglycan (DAG1)) and rabbit anti-CD147 antibody were purchased from Sino Biological Europe GmbH (Eschborn, Germany).

HiPSCs Culture: All experiments using human induced pluripotent stem cells were performed according to the ethical principles of Karlsruhe Institute of Technology. The hiPSCs (D1 line, kindly provided by Prof. Dr. Martin Bastmeyer) were routinely cultured on LDEV-free Matrigel-coated 6-well plates with serum-free, chemically well-defined mTeSR™ plus medium supplemented with 1 μ g mL⁻¹ doxycycline and 50 μ g mL⁻¹ normocin at 37 °C in a humidified 5% CO₂ incubator. Before passaging, cells were washed with fresh DMEM/F12 medium three times. Then 10–20 cell clumps were mechanically dissociated from hiPSCs colonies using a sterilized Pasteur pipette and the clumps were transferred onto another freshly Matrigel coated well plate surface. Thereafter, the cells were mechanically cleaned and the medium was changed every day. Cells were passaged every 5–7 days. For obtaining small cell clusters, hiPSCs colonies were treated with a commercial cell detaching reagent ReLeSR™ according to the manufacturer's instructions. The hiPSCs cultured with mTeSR medium with Matrigel and without Matrigel were set as positive and negative control, respectively.

Droplet Microarrays (DMA): DMA slides with 1 mm side length square spots (catalogue number: G-np-102) were purchased from Aquaray GmbH (Eggenstein-Leopoldshafen, Germany). Each DMA slide contains 672 individual spots with side length of 1 mm and 500 μ m distance between the side of square spot. All the experiments were performed on these DMAs. The DMAs were sterilized by immersing in absolute ethanol for 60 min and ensured drying on the cell culture bench before using.

hiPSCs Culture on DMAs: First, the 1% Matrigel in mTeSR™ plus medium was printed with a volume of 60 nL per spot by I-Dot One dispenser (Dispentix, Stuttgart, Germany). The printing started once the hu-

midity reached 70%. The DMA slide was then placed in a Petri dish which was sealed with parafilm at RT for 1 h to allow the Matrigel coating. For automated printing, hiPSCs cells were detached and printed onto Matrigel pre-coated DMA slides with a volume of 200 nL per spot. For manual seeding, DMA slide was placed into a Petri dish and 1.5 mL cell suspension was applied and incubated for 30 s. Afterwards, the Petri dish was slightly tilted to let the big droplet of cell suspension roll off the slide, resulting in spontaneous cellular droplet array formation. Then, the cell containing slides (manual seeding and automated printing) were placed into Petri dishes with wetted humidifying pads in the upper lid and 2 mL PBS below. The cells were cultured on DMA for 24 h without medium change. For negative control, cells were directly printed onto each individual spot without Matrigel coating.

Imaging: The DMA slides were placed into Petri dishes or 4-well rectangular dishes (Nunc, Thermo Fisher Scientific Inc, MA, USA) for imaging. The images were taken by both fluorescence microscope Keyence BZ-9000 (KEYENCE, Osaka, Japan) and Olympus IX81 inverted motorized microscope (Olympus, Tokyo, Japan) with 10x magnification for three channels (bright field, red fluorescence channel for PI staining and green fluorescence channel for Calcein AM staining). The IF staining images were taken by confocal laser scanning microscope Leica TCS SPE (Leica, Mannheim, Germany) with 40x magnification and confocal laser scanning microscope Zeiss LSM 800 with 10x and 25x magnification (Zeiss, Oberkochen, Germany).

Cell Viability Assay: The viability of hiPSCs cultured on DMA was investigated by the live–dead staining. Calcein AM and PI were used to stain live and dead cells, respectively. Calcein AM is a fluorogenic esterase substrate that is hydrolyzed to a green-fluorescent product (Calcein), producing a fluorescent green in cytosol of living cells. While PI can pass through damaged membranes of dead cells and binds with DNA, which indicates dead cells in red fluorescence. Briefly, 200 nL of hiPSCs cell suspension was added into each spot after 60 nL 1% Matrigel solution coating. At 24 h after incubation, 75 nL of Calcein AM/PI mixture was printed into each spot to reach a final concentration of 0.5 $\mu\text{g mL}^{-1}$ for both Calcein AM and PI. Then the DMA slides were placed in 37 °C for 15 min before imaging by fluorescence microscope Keyence BZ-9000 and Olympus IX81 inverted motorized microscope with 10x magnification. The area of Calcein AM and PI positive were analyzed by ImageJ.^[52] The cell viability was calculated as Calcein AM positive area to the sum of Calcein AM and PI positive area. The same live–dead staining procedure was applied to the manual seeding method cell viability investigation.

Primary Screening: The proteins (Thy-1, EphB4, EphA1, E-cadherin, CAR, JAM1, EpCAM, BSG, DAG1, HA, and Laminin 521 were individually diluted to 10, 20, and 30 $\mu\text{g mL}^{-1}$ in 1x PBS +/+ and combined to reach the screening concentration of each protein to 10 $\mu\text{g mL}^{-1}$. Then the protein solutions were printed onto DMA spots using I-Dot One dispenser with 60 nL per spot. Then the DMA slides were placed in a 10 cm parafilm sealed Petri dish and placed at RT for 2 h to allow proteins coating on the droplet surface. The hiPSCs cell suspension was then printed onto coated spots and grown on DMA for 24 h before fixation and staining for NANOG expression. Images were acquired using an inverted fluorescence microscope. The mean fluorescence intensity of images was then automatically analyzed using MATLAB.

Immunofluorescence (IF) Staining: The cells were fixed with 4% formaldehyde solution in PBS and permeabilized with 0.5% Triton X-100 at RT for 15 min. Afterwards, the cells were washed with fresh PBS and incubated with 1% BSA buffer at 37 °C for 1 h to block nonspecific binding. The cells were incubated with following primary antibodies: rabbit anti-OCT-4A, rabbit anti-SOX2, rabbit anti-NANOG, mouse anti-SSEA4, mouse anti-TRA-1-60(S), mouse anti-TRA-A-81, and rabbit anti-E-cadherin at 4 °C overnight. The second day, the cells were washed with fresh PBS and then incubated with corresponding secondary antibodies: Alexa Fluor® 488 goat anti rabbit IgG H&L and Alexa Fluor® 594 goat anti mouse IgG H&L in the dark for 1 h at RT. Nuclei were counterstained with DAPI at 37 °C for 15 min. The same procedure was applied for E-Cadherin, phalloidin, FOXA2, brachyury, and β -Tubulin3 staining except the antibodies were replaced by corresponding antibody solution and phalloidin staining solution.

Colony Attachment Efficiency: The “hit” proteins were applied to coat 12-well plates at RT for 2 h with the concentration of 10 $\mu\text{g mL}^{-1}$. The protein solution was aspirated and hiPSCs were then detached by ReLeSR™ and added into each well. Cell attachment were visually scored by counting attached colony numbers in five random selected fields in each technically repeated well on day 1, 2, 3, and 4. Experiments were repeated three times. The average of the attached colony numbers of protein groups were compared with that of Matrigel to assess the colony attachment ability of “hits” from the screening.

Long-Term Culture Validation: HiPSCs were mechanically dissociated and 10–20 colonies were transferred to the pre-coated plates. Then the cells were manually cleaned together with daily medium change. The cells were passaged every 3–5 days under the same conditions for five passages. HiPSCs culture on MG-coated plates were used as a control. The morphology of hiPSCs at each passage was acquired by an inverted microscope and pluripotency at each passage was investigated by IF staining of NANOG expression. After five passages, the hiPSCs were stained for six pluripotency markers (SOX2, OCT-4A, NANOG, TRA-1-60, SSEA4, and TRA-1-81).

Real-Time PCR (qPCR): Pluripotency gene expression was quantified using qPCR analysis. Total cellular RNA was isolated by RNeasy Mini kit, according to manufacturer’s protocol. cDNA was synthesized according to the usual protocol by Superscript IV kit for reverse transcription. Real-time PCR was performed on a StepOne Real-time PCR system (Life Technologies GmbH, Germany), after processing the cDNA samples with Gotaq qPCR master mix. Real-time data was analyzed as described.^[53] Primer sequences had been provided in Table S2 (Supporting Information). Data was normalized to glyceraldehyde 3-phosphate dehydrogenase (GAPDH) expression and statistical differences between groups were analyzed by unpaired *t*-test.

Three Germ Layers Differentiation: To induce embryoid body (EB) formation, hiPSCs colonies were dissociated and collected after five passages on “hit” protein coatings. Then cells were seeded as 25 μL per drop on the lid of a 10 cm Petri dish. The lid was then inverted to close the Petri dish with 10 mL PBS below in the Petri dish. The hanging droplets contained Petri dish was then placed for 48 h to allow the formation of EBs. The formed EBs were then transferred onto gelatin coated well-plates and cultured in DMEM medium supplemented with 15% FBS and 1% Pen/Strep for additional 14 days to induce spontaneous differentiation into three-germ layers (endoderm, mesoderm, and ectoderm). Then IF staining experiments were conducted as described above with anti-FOXA2/HNF-3 β (endoderm), anti-Brachyury (mesoderm), and anti- β -Tubulin3 (ectoderm) antibodies.

Statistical Analysis: The statistical analysis of the mean brightness was performed using MATLAB R2018a (The MathWorks, USA). In the fluorescence images borders were cropped, and a segmentation using the 95th percentile of pixel brightness values as threshold was done. Found structures were optimized using morphological operators (opening ($r = 7$), hole-filling). All remaining objects were quantified by their area and their brightness above background (set as minimum brightness in the image).

The robustness and feasibility of the screening was evaluated prior to the screening by calculation of the Z-factor (Z') between positive and negative controls according to the following equations:

$$Z' = 1 - \frac{(3\sigma_{c+} + 3\sigma_{c-})}{|\mu_{c+} - \mu_{c-}|} \quad (2)$$

where σ = standard deviation (SD) of brightness, μ = mean of brightness, $c+$ = positive control, and $c-$ = negative control.

In the primary screening, the mean fluorescence intensity representing NANOG expression level in hiPSCs cultured on each protein coating was then analyzed and normalized against the intensity of cells cultured on positive control coatings (MG⁺ spots). All the experiments were repeated at least three times. Data were presented as mean \pm SD or mean \pm SEM. The statistical significance of the experimental data was analyzed with a two-tailed Student *t*-test using GraphPad Prism 9 software for windows. The *p*-value threshold for statistical significance set at **p* < 0.05, ***p* < 0.01 and ****p* < 0.001.

Supporting Information

Supporting Information is available from the Wiley Online Library or from the author.

Acknowledgements

The research was supported by DFG (Heisenbergprofessur Projektnummer: 406232485, LE2936/9-1). The work was further supported by the Helmholtz program "Materials Systems Engineering". The Chinese Scholarship Council (fellowship to Y.L.) is also gratefully acknowledged. The authors also thank Dr. Shraddha Chakraborty for help with qPCR. PAL, MB, and SB thank Germany's Excellence Strategy 2082/1-390761711 (Excellence Cluster "3D Matter Made to Order"). PAL and MB appreciate the Deutsche Forschungsgemeinschaft (DFG, German Research Foundation).

Open access funding enabled and organized by Projekt DEAL.

Conflict of Interest

Both P.A.L and A.A.P are stakeholders of Aquarray GmbH, from which slides were used in this study. Other co-authors declare no conflict of interests.

Data Availability Statement

The data that support the findings of this study are available from the corresponding author upon reasonable request.

Keywords

droplet microarrays, high-throughput screening, hiPSCs, pluripotency, xeno-free

Received: March 31, 2022

Revised: June 10, 2022

Published online:

- [1] K. Takahashi, K. Tanabe, M. Ohnuki, M. Narita, T. Ichisaka, K. Tomoda, S. Yamanaka, *Cell* **2007**, *131*, 861.
- [2] a) S. Dakhore, B. Nayer, K. Hasegawa, *Stem Cells Int.* **2018**, *2018*, 7396905; b) N. Moriarty, C. W. Gantner, C. P. J. Hunt, C. M. Ermine, S. Frausin, S. Viventi, D. A. Ovchinnikov, D. Kirik, C. L. Parish, L. H. Thompson, *Cell Stem Cell* **2022**, *29*, 434.
- [3] R. G. Rowe, G. Q. Daley, *Nat. Rev. Genet.* **2019**, *20*, 377.
- [4] A. Cota-Coronado, P. B. Ramirez-Rodriguez, E. Padilla-Camberos, E. F. Diaz, J. M. Flores-Fernandez, D. Avila-Gonzalez, N. E. Diaz-Martinez, *Drug Discovery Today* **2019**, *24*, 334.
- [5] K. Makino, M. Long, R. Kajihara, S. Matsueda, T. Oba, K. Kanehira, S. Liu, F. Ito, *J. Immunother. Cancer* **2022**, *10*, e003827.
- [6] P. Ghasemi-Dehkordi, M. Allahbakhshian-Farsani, N. Abdian, A. Mirzaeian, J. Saffari-Chaleshtori, F. Heybati, G. Mardani, A. Karimi-Taghanaki, A. Doosti, M. S. Jami, M. Abolhasani, M. Hashemzadeh-Chaleshtori, *J. Cell Commun. Signal.* **2015**, *9*, 233.
- [7] K. Chen, B. Mallon, R. D. G. McKay, P. G. Robey, *Cell Stem Cell* **2014**, *14*, 13.
- [8] I. Ullah, J. F. Busch, A. Rabien, B. Ergun, C. Stamm, C. Knosalla, S. Hippenstiel, P. Reinke, A. Kurtz, *Adv. Sci.* **2020**, *7*, 1901198.
- [9] D. Marotta, C. Rao, V. Fossati, *Human Induced Pluripotent Stem Cell (iPSC) Handling Protocols: Maintenance, Expansion, and Cryopreservation*, Springer, New York, NY **2021**.
- [10] E. A. Aisenbrey, W. L. Murphy, *Nat. Rev. Mater.* **2020**, *5*, 539.
- [11] a) T. Sung, H. Li, A. Higuchi, S. S. Kumar, Q. Ling, Y. Wu, T. Burnouf, M. Nasu, A. Umezawa, K. F. Lee, H. Wang, Y. Chang, S. T. Hsu, *Biomaterials* **2020**, *230*, 119638; b) Y. Deng, S. Wei, L. Yang, W. Yang, M. S. Dargusch, Z. Chen, *Adv. Funct. Mater.* **2018**, *28*, 1705546; c) A. Higuchi, A. H. Hirad, S. S. Kumar, M. A. Munusamy, A. A. Alarfaj, *Acta Biomater.* **2020**, *116*, 162.
- [12] L. Li, S. A. L. Bennett, L. Wang, *Cell Adhes. Migr.* **2012**, *6*, 59.
- [13] M. Caiazza, Y. Okawa, A. Ranga, A. Piersigilli, Y. Tabata, M. P. Lutolf, *Nat. Mater.* **2016**, *15*, 344.
- [14] a) Y. Chen, L. Chen, M. Li, H. Li, A. Higuchi, S. S. Kumar, Q. Ling, A. A. Alarfaj, M. A. Munusamy, Y. Chang, G. Benelli, K. Murugan, A. Umezawa, *Sci. Rep.* **2017**, *7*, 45146; b) M. D'Antonio, G. Woodruff, J. L. Nathanson, A. D'Antonio-Chronowska, A. Arias, H. Matsui, R. Williams, C. Herrera, S. M. Reyna, G. W. Yeo, L. S. B. Goldstein, A. D. Panopoulos, K. A. Frazer, *Stem Cell Rep.* **2017**, *8*, 1101.
- [15] a) C. Bock, E. Kiskinis, G. Verstappen, H. Gu, G. Boulting, Z. D. Smith, M. Ziller, G. F. Croft, M. W. Amoroso, D. H. Oakley, A. Gnirke, K. Eggan, A. Meissner, *Cell* **2011**, *144*, 439; b) R. L. Gundry, D. R. Rioridon, Y. Tarasova, S. Chuppa, S. Bhattacharya, O. Juhasz, O. Wiedemeier, S. Milanovich, F. K. Noto, I. Tchernyshyov, K. Raginski, D. Bausch-Fluck, H. J. Tae, S. Marshall, S. A. Duncan, B. Wollscheid, R. P. Wersto, S. Rao, J. E. Van Eyk, K. R. Boheler, *Mol. Cell. Proteomics* **2012**, *11*, 303; c) J. C. Ardila Riveros, A. K. Blöching, S. Atwell, M. Mousus, N. Compera, O. Rajabnia, T. Georgiev, H. Lickert, M. Meier, *Lab Chip* **2021**, *21*, 4685; d) A. Sharma, W. Burridge Paul, L. McKeithan Wesley, R. Serrano, P. Shukla, N. Sayed, M. Churko Jared, T. Kitani, H. Wu, A. Holmström, E. Matsa, Y. Zhang, A. Kumar, C. Fan Alice, C. del Álamo Juan, M. Wu Sean, J. Moslehi Javid, M. Mercola, C. Wu Joseph, *Sci. Transl. Med.* **2017**, *9*, eaaf2584.
- [16] Y. Mei, K. Saha, S. R. Bogatyrev, J. Yang, A. L. Hook, Z. I. Kalciglu, S. W. Cho, M. Mitalipova, N. Pyzocha, F. Rojas, K. J. Van Vliet, M. C. Davies, M. R. Alexander, R. Langer, R. Jaenisch, D. G. Anderson, *Nat. Mater.* **2010**, *9*, 768.
- [17] A. D. Celiz, J. G. W. Smith, A. K. Patel, A. L. Hook, D. Rajamohan, V. T. George, L. Flatt, M. J. Patel, V. C. Epa, T. Singh, R. Langer, D. G. Anderson, N. D. Allen, D. C. Hay, D. A. Winkler, D. A. Barrett, M. C. Davies, L. E. Young, C. Denning, M. R. Alexander, *Adv. Mater.* **2015**, *27*, 4006.
- [18] a) R. G. Ireland, M. Kibschull, J. Audet, M. Ezzo, B. Hinz, S. J. Lye, C. A. Simmons, *Biomaterials* **2020**, *248*, 120017; b) D. A. Brafman, K. D. Shah, T. Fellner, S. Chien, K. Willert, *Stem Cells Dev.* **2009**, *18*, 1141; c) D. A. Brafman, S. Chien, K. Willert, *Nat. Protoc.* **2012**, *7*, 703.
- [19] Y. Liu, T. Tronser, R. Peravali, M. Reischl, P. A. Levkin, *Adv. Biosyst.* **2020**, *4*, 1900257.
- [20] T. Tronser, K. Demir, M. Reischl, M. Bastmeyer, P. A. Levkin, *Lab Chip* **2018**, *18*, 2257.
- [21] A. A. Popova, D. Marcato, R. Peravali, I. Wehl, U. Schepers, P. A. Levkin, *Adv. Funct. Mater.* **2018**, *28*, 1703486.
- [22] a) H. Cui, X. Wang, J. Wesslowski, T. Tronser, J. Rosenbauer, A. Schug, G. Davidson, A. A. Popova, P. A. Levkin, *Adv. Mater.* **2021**, *33*, 2006434; b) A. A. Popova, T. Tronser, K. Demir, P. Haitz, K. Kuodyte, V. Starkuviene, P. Wajda, P. A. Levkin, *Small* **2019**, *15*, 1901299.
- [23] M. Benz, M. R. Molla, A. Boser, A. Rosenfeld, P. A. Levkin, *Nat. Commun.* **2019**, *10*, 2879.
- [24] M. Brehm, S. Heissler, S. Afonin, P. A. Levkin, *Small* **2020**, *16*, 1905971.
- [25] T. Liu, X. Zeng, F. Sun, H. Hou, Y. Guan, D. Guo, H. Ai, G. Zhang, W. Wang, *Cell. Physiol. Biochem.* **2017**, *41*, 819.
- [26] S. Miura, A. Suzuki, *Cell Stem Cell* **2017**, *21*, 456.
- [27] H. W. Leung, C. O. N. Leung, E. Y. Lau, K. P. S. Chung, E. H. Mok, M. M. L. Lei, R. W. H. Leung, V. W. Keng, C. Ma, Q. Zhao, I. O. L. Ng, S. Ma, T. K. Lee, *Cancer Res.* **2021**, *81*, 3229.

- [28] Y. Sugawara, K. Hamada, Y. Yamada, J. Kumai, M. Kanagawa, K. Kobayashi, T. Toda, Y. Negishi, F. Katagiri, K. Hozumi, M. Nomizu, Y. Kikkawa, *Sci. Rep.* **2019**, *9*, 13037.
- [29] S. He, H. Sun, L. Lin, Y. Zhang, J. Chen, L. Liang, Y. Li, M. Zhang, X. Yang, X. Wang, F. Wang, F. Zhu, J. Chen, D. Pei, H. Zheng, *J. Biol. Chem.* **2017**, *292*, 18542.
- [30] N. S. Pripuzova, M. Getie-Kehtie, C. Grunseich, C. Sweeney, H. Malech, M. A. Alterman, *Stem Cell Res.* **2015**, *14*, 323.
- [31] A. Domogatskaya, S. Rodin, K. Tryggvason, *Annu. Rev. Cell Dev. Bi.* **2012**, *28*, 523.
- [32] A. Laperle, C. Hsiao, M. Lampe, J. Mortier, K. Saha, S. P. Palecek, K. S. Masters, *Stem Cell Rep.* **2015**, *5*, 195.
- [33] A. Troster, S. Heinzlmeir, B. T. Berger, S. L. Gande, K. Saxena, S. Sreeramulu, V. Linhard, A. H. Nasiri, M. Bolte, S. Muller, B. Kuster, G. Medard, D. Kudlinski, H. Schwalbe, *ChemMedChem* **2018**, *13*, 1629.
- [34] E. Parisini, J. M. G. Higgins, J. Liu, M. B. Brenner, J. Wang, *J. Mol. Biol.* **2007**, *373*, 401.
- [35] M. J. van Raaij, E. Chouin, H. van der Zandt, J. M. Bergelson, S. Cusack, *Structure* **2001**, *9*, 1.
- [36] A. E. Prota, J. A. Campbell, P. Schelling, J. C. Forrest, M. J. Watson, T. R. Peters, M. Aurrand-Lions, B. A. Imhof, T. S. Dermody, T. Stehle, *Proc. Natl. Acad. Sci. U.S.A.* **2003**, *100*, 5366.
- [37] M. Pavsic, G. Guncar, K. Djinovic-Carugo, B. Lenarcic, *Nat. Commun.* **2014**, *5*, 4764.
- [38] X. Yu, T. Hu, J. Du, J. Ding, X. Yang, J. Zhang, B. Yang, X. Shen, Z. Zhang, W. Zhong, N. Wen, H. Jiang, P. Zhu, Z. Chen, *J. Biol. Chem.* **2008**, *283*, 18056.
- [39] S. Covaceuszach, M. Bozzi, M. G. Bigotti, F. Sciandra, P. V. Konarev, A. Brancaccio, A. Cassetta, *FEBS Open Bio* **2017**, *7*, 1064.
- [40] P. Teriete, S. Banerji, M. Noble, C. D. Blundell, A. J. Wright, A. R. Pickford, E. Lowe, D. J. Mahoney, M. I. Tammi, J. D. Kahmann, I. D. Campbell, A. J. Day, D. G. Jackson, *Mol. Cell* **2004**, *13*, 483.
- [41] M. Takizawa, T. Arimori, Y. Taniguchi, Y. Kitago, E. Yamashita, J. Takagi, K. Sekiguchi, *Sci. Adv.* **2017**, *3*, e1701497.
- [42] P. Navarro, N. Festuccia, D. Colby, A. Gagliardi, N. P. Mullin, W. Zhang, V. Karwacki-Neisius, R. Osorno, D. Kelly, M. Robertson, I. Chambers, *EMBO J.* **2012**, *31*, 4547.
- [43] M. Ohgushi, M. Matsumura, M. Eiraku, K. Murakami, T. Aramaki, A. Nishiyama, K. Muguruma, T. Nakano, H. Suga, M. Ueno, T. Ishizaki, H. Suemori, S. Narumiya, H. Niwa, Y. Sasai, *Cell Stem Cell* **2010**, *7*, 225.
- [44] Y. Liu, S. Chakraborty, C. Direksilp, J. M. Scheiger, A. A. Popova, P. A. Levkin, *Mater. Today Bio* **2021**, *12*, 100153.
- [45] a) A. Filipczyk, C. Marr, S. Hastreiter, J. Feigelman, M. Schwarzfischee, P. S. Hoppe, D. Loeffler, K. D. Kokkiliaris, M. Endeke, B. Schaubberger, O. Hilsenbeck, S. Skylaki, J. Hasenauer, K. Anastasiadis, F. J. Theis, T. Schroeder, *Nat. Cell Biol.* **2015**, *17*, 1235; b) E. Abranches, A. M. V. Guedes, M. Moravec, H. Maamar, P. Svoboda, A. Raj, D. Henrique, *Development* **2014**, *141*, 2770; c) P. Navarro, N. Festuccia, D. Colby, A. Gagliardi, N. P. Mullin, W. S. Zhang, V. Karwacki-Neisius, R. Osorno, D. Kelly, M. Robertson, I. Chambers, *EMBO J.* **2012**, *31*, 4547.
- [46] J. H. Zhang, T. D. Y. Chung, K. R. Oldenburg, *J. Biomol. Screen.* **1999**, *4*, 67.
- [47] E. Narva, A. Stubb, C. Guzman, M. Blomqvist, D. Balboa, M. Lerche, M. Saari, T. Otonkoski, J. Ivaska, *Stem Cell Rep.* **2017**, *9*, 67.
- [48] N. Malo, J. A. Hanley, S. Cerquozzi, J. Pelletier, R. Nadon, *Nat. Biotechnol.* **2006**, *24*, 167.
- [49] S. Rodin, A. Domogatskaya, S. Ström, E. M. Hansson, K. R. Chien, J. Inzunza, O. Hovatta, K. Tryggvason, *Nat. Biotechnol.* **2010**, *28*, 611.
- [50] S. Rodin, L. Antonsson, C. Niaudet, O. E. Simonson, E. Salmela, E. M. Hansson, A. Domogatskaya, Z. Xiao, P. Damdimopoulou, M. Sheikhi, J. Inzunza, A.-S. Nilsson, D. Baker, R. Kuiper, Y. Sun, E. Blennow, M. Nordenskjöld, K.-H. Grinnemo, J. Kere, C. Betsholtz, O. Hovatta, K. Tryggvason, *Nat. Commun.* **2014**, *5*, 3195.
- [51] H. Kurosawa, *J. Biosci. Bioeng.* **2007**, *103*, 389.
- [52] C. A. Schneider, W. S. Rasband, K. W. Eliceiri, *Nat. Meth.* **2012**, *9*, 671.
- [53] M. W. Pfaffl, *Nucleic Acids Res.* **2001**, *29*, 45e.